One plausible reason for the change in ENSO characteristics in the 2000s

Vladimir N. Stepanov[1]

vlnst@hotmail.co.uk

Abstract

It is well known that El Niño Southern Oscillation (ENSO) causes floods, droughts in different regions of the Earth and the collapse of fisheries in the tropical Pacific, therefore forecasting of ENSO is an important task in climate researches. Variations in the equatorial warm water volume of the tropical Pacific and wind variability in the western equatorial Pacific has been considered to be a good ENSO predictor. However, in the 2000s, the interrelationship between these two characteristics and ENSO onsets became weak. This article attempts to find some plausible explanation for this.

The results presented here demonstrate a possible link between the variability of atmospheric conditions over the Southern Ocean and their impact on the ocean circulation leading to the amplifying of ENSO events. It is shown that the variability of the atmospheric conditions upstream of Drake Passage can strongly influence ENSO events. The interrelationship between ENSO and variability in the equatorial warm water volume of the equatorial Pacific, together with wind variability in the western equatorial Pacific has recently weakened. It can be explained by the fact that the process occurred in the Southern Ocean recently became a major contributor amplifying ENSO events (in comparison with the processes of interaction between the atmosphere and the ocean in the tropics of the Pacific). Likely it is due to a warmer ocean state observed from the end of the 1990s that led to smaller atmospheric variability in the tropics and insignificant their changes in the Southern Ocean.

Keywords: ENSO; the Southern Ocean; numerical modelling.

---

[1] This work has been carried out while the author was working at Department of Meteorology, University of Reading

1. Introduction

Forecasting of ENSO events is an important task in climate research because ENSO events have a global influence weather systems: both in the tropical Pacific (where the ENSO events occur) and at moderate/high latitudes (e.g., Lau et al. (2005), Nicholls et al. (2005), Mokhov and Smirnov (2006), Müller and Roecker (2006), Stepanov et al. 2012, demonstrated the influence of warm ENSO on the weather in the Northern Hemisphere). Many publications provide evidence that the interactions between high latitudes and the tropics also can impact the ENSO variability (e.g., Pierce et al. (2000), Vimont et al. (2003), Dong et al. (2006), Chang et al. (2007), Alexander et al. (2008), Wang et al. (2012), Terray (2011)).

As was noted by Stepanov (2009 a, b), the above mentioned teleconnections can be explained by the fact that ENSO events could be considered as a consequence of changes in the global meridional atmospheric circulation rather than a local phenomenon in the tropics. The link between the tropics and high latitudes can exist due to interactions between the tropics and the mid-latitudes, which influence the high latitudes and vice versa. For example, warming (cooling) of the upper ocean layer in the tropics (which can be related, for example, to the seasonal cycle, or consequence of the frequent occurrence of the weak El Niño) leads to an increase (decrease) in the warming of the troposphere in a region where atmospheric mass upwells (the Pacific Ocean is the largest ocean and therefore has the largest contribution to these changes). This means that warmer (colder) upgoing air from the tropical zone is transported by the Hadley circulation cell to the subtropics, which slows down (accelerates) the air motion in the downwelling branch of the Hadley cell and then leads to weakening (intensification) of the wind in the mid-latitudes, which then lead to similar changes in the high latitudes. Therefore many teleconnections between ENSO and weather at distant regions from the tropical Pacific have been found, and the paper will pay an attention to the link between the wind processes over the Antarctic Circumpolar Current (ACC) and ENSO events (Stepanov, 2009a,b).

The intensity of Walker circulation is associated with the Southern Oscillation Index (SOI) that describes fluctuations in the difference of the surface air pressure anomalies between Tahiti (17º52'S) and Darwin (12°25'S). During warm ENSO conditions there is an eastward displacement of the Walker circulation, resulting in high atmospheric pressure and cooler SST conditions over the western Pacific. During cold ENSO conditions there is an intensification of normal Walker circulation conditions, producing low atmospheric pressure and warmed SSTs in the western Pacific (http://www.bom.gov.au/lam/climate/levelthree/analclim/elnino.htm). Thus, the SOI can be considered as atmospheric component of ENSO due to the variability of atmospheric forcing in the western equatorial Pacific. Fig. 1a shows 1989-2008 correlations of zonally averaged monthly sea level pressure (SLP) with SOI-index taken with negative sign, which was taken from http://www.cpc.ncep.noaa.gov/data/indices. We clearly see seasonality and that SOI-index leads the SLP change in low latitudes. However, as Fig. 1 (b-d) demonstrates, the change of the zonally averaged SLP occurs in phase with the change of the meridional gradient of the SLP. Likely the meridional gradient change of the SLP is a primary source of the SLP variability in the low latitudes that then in its turn, results in to the next SLP change in the tropics in the zonal direction, i.e. SOI index change (Fig. 1a). The above figures show that even for annual cycle the change of the meridional gradient of the atmospheric pressure in low latitudes is more important for the variability of atmospheric pressure here than SOI-index variability, since the correlations of zonally averaged SLP with the meridional gradient of the atmospheric pressure is higher and the last can lead the variability of the zonally averaged SLP, which, in its turn, can impact the meridional gradient of the SLP. After removing the seasonal cycle and low-pass filtering with periods longer than 18 months, the correlation between SOI-index and zonally averaged sea level pressure difference between 17° and 12°S (Fig. 1d) is about -0.6 (all the correlations presented by the paper are statistically significant with a probability of 95%, which was determined through the effective number of degrees of freedom following Bretherton et al. (1999)). According to the absolute values of correlation coefficients between NINO and SOI indexes (≤0.7), less than 50% of the NINO variability can be explained by changes of atmospheric forcing in the western equatorial Pacific. Thus, it is likely that the development of ENSO events can be due to some other mechanism, e.g. the global meridional atmospheric circulation change that can affect both high and low latitudes. Thus we can assume that the changes in the global meridional atmospheric circulation begun in April (i.e. time when the initiation of ENSO begins) can lead to the changes both in the tropics and in the Southern ocean simultaneously, and some link between atmospheric processes in the Southern ocean and ENSO can exist (Stepanov (2009a).

Numerical experiments presented by Stepanov (2009 a,b) have demonstrated that the variability of wind forcing over the ACC, together with the effect of bottom topography, lead to the appearance of anomalies in pressure and density in the Southern Ocean. The appearance of these anomalies is caused by the short time scale variability of the meridional mass fluxes in the Pacific sector of the Southern Ocean north of 47°S, of which the average value from July to September is estimated to be greater than 2000 Gt (1 Gt $=10^9$t). This variability of the oceanic mass in the Pacific Ocean is negatively significantly correlated with the wind forcing over the ACC. As a measure of wind strength the SAM index (Southern Hemisphere Annular Mode) has been used. This is determined as the normalized difference between the zonal-mean SLP between 40°S and 70°S (obtained from the National Oceanic and Atmospheric Administration).

The density anomalies near the regions, where the strong variability of the meridional mass fluxes in the Pacific sector of the Southern Ocean is observed, can be transported to the low latitudes of the Pacific Ocean by means of the wave mechanism described by Ivchenko et al. (2004, 2006) and Blaker et al (2006). Here they interact with the stratification and can cause variations in the inclination of the thermocline in the tropical Pacific, which, in turn, can facilitate more intense development of ENSO effects (Stepanov, (2009 a,b)). Therefore there is also high correlation (with coefficient of ~0.8) between the variability of the oceanic mass in the Pacific Ocean and ENSO events (Stepanov, 2009 a).

The above mentioned variability of the meridional mass fluxes in the Pacific sector of the Southern Ocean is due to mass exchange occurring between the Southern Ocean and Pacific regions at periods of 30–100 days, which is determined by the balance of wind stress by form stress (a pressure difference across topographic obstacles) in Drake Passage, together with the inverse barometer response to atmospheric pressure (see details in Stepanov and Hughes (2006)).

This paper puts forward the plausible explanation why we see the breakdown in the 2000s of ENSO predictors proposed by McPhaden (2003). In accordance with the recharge/discharge paradigm for ENSO (see, for example, Jin (1997)), McPhaden, (2003, 2006), found some ENSO precursors in observation data: it was shown that variation in the equatorial warm water volume of the tropical Pacific and wind variability in the western equatorial Pacific precedes ENSO by two to three seasons and can be a useful ENSO predictor. A similar approach was proposed by Clarke and Van Gorder, (2003) who used zonal wind stress over the Indo-Pacific tropics.

However Horii et al. (2012) have shown that the robust predictability of these predictors for ENSO has changed in the 2000s. Before 2000, during two decades, the increase/decrease of the warm water volume of the equatorial Pacific (recharge/discharge phase of the recharge/discharge oscillator) together with strong/weak wind in the western equatorial Pacific preceded warm (El Niño) and cold (La Niña) ENSO events by two to three seasons. While in the 2000s, the interrelationship between these predictors and following ENSO became weak, especially for the ENSO events after 2005. According to Horii et al. (2012) these changes may be caused by frequent occurrences of the “warm-pool El Niño”, which is characterized by SST anomalies centered in the central equatorial Pacific (Larkin and Harrison (2005), Ashok et al. (2007), Kao and Yu (2009), Kug et al. (2009), and Lee and McPhaden, (2010)), compared with that during 1980-2000. Under these conditions, the tropical temperature anomalies are weak and the discharge phase of the recharge/discharge oscillator is not significant. Therefore the frequent occurrence of the warm-pool El Niño in the 2000s cannot provide discharged conditions that prevent the development of significant cold ENSO events.

No reasons have been mentioned by Horii et al. (2012) to explain why the conventional ENSO events have been recently displaced by the "warm-pool El Niño". The comparison of the time series of the NINO3 (SST averaged in area of 5°N-5°S; 150°W-90°W) and NINO4 (SST averaged in area of 5°N-5°S; 160°E-150°W) indexes (www.cpc.ncep.noaa.gov/data/indices), as a measure of the departure from normal sea surface temperature in the east and central Pacific Ocean respectively (not shown), demonstrates that both indexes are varied almost in phase, but the amplitudes of the variability are different: the amplitude of NINO3 index can be up to 2 times larger (before 2000) than NINO4. It is reasonable to think that NINO4 describes a primary source of some factor forcing the onset of ENSO events (that exists and after 2000), while NINO3 is a combination effect of the primary source and changes due to the beginning of ENSO onset in the central Pacific, i.e. the subsequent interaction between the atmosphere and ocean in the tropics (that has changed/modified after 2000). It is likely that the subsequent changes in the Walker circulation cell could significantly amplify ENSO development in this region located close to land prior to the 2000s. The results presented in this article will lead us to the conclusion that the wind processes over the ACC, and particularly the atmospheric conditions upstream of Drake Passage, can strongly influence the ENSO events (i.e. we should pay an attention to non-tropical factor too).

Section 2 describes the typical changes in the atmospheric conditions over the Southern Ocean a few months before the maximum phase of the development of ENSO and how these changes can be interrelated with ENSO events. Also the results of an empirical orthogonal function (EOF) analysis are presented in Section 3 to identify modes of variability relevant to the hypothesis that processes occurring in the Southern Ocean can amplify ENSO events. Section 4 provides some discussion and conclusions about the link between the atmospheric and oceanic processes in the Southern Ocean and the maximum phase of the development of ENSO events.

2. Is the Southern Ocean a main trigger for the development of the maximum phase of ENSO during warm periods?

As was mentioned early, the variability of the oceanic mass in the Pacific sector of the Southern ocean is negatively correlated with the wind forcing over the ACC. We will see later that the wind weakness is due to atmospheric pressure pattern blocking over the south-east Pacific. The change of atmospheric conditions over the ACC, and particularly over the region upstream of Drake Passage, can substantially influence the bottom pressure on the western side of Drake Passage and the balance between wind stress and form stress in Drake Passage, which can impact the variability of the meridional mass fluxes in the Pacific sector of the Southern Ocean, and hence ENSO events.

It is well known that the maximum phase of the development of the warm/cold ENSO events is observed in November-December, while the ENSO onset, i.e. time when the initiation of ENSO begins, is observed around April to June in many cases (e.g. Larkin and Harrison (2005)). Stepanov (2009 a,b) has shown that there is a time lag of 4–6 months between the variation of the oceanic mass in the Pacific sector of the Southern ocean in the winter–spring season of the Southern Hemisphere and the maximum phase of ENSO development (which is determined by the time needed to transport the density anomalies appearing in the Southern Ocean to low latitudes by means of a wave mechanism described by Ivchenko et al. (2004, 2006)). Therefore, we have to pay attention to the atmospheric variability over the ACC that occurred about 4 months before the maximum phase of ENSO development, i.e. we will analyze what factors can impact the development of the maximum phase of ENSO in the end of the year.

Figures 2a-b show 1989-2011 mean SLP and its standard deviation. One can see that the field of SLP has almost zonal structure over the ACC, while upstream of Drake Passage there is a high variability of SLP. It means that sometimes in this region instead of a usual low atmospheric pressure, an anticyclonic/cyclonic atmospheric circulation pattern can occur.

From correlation between the monthly average SAM index and SLP (Fig. 2c) one can see that the wind strength over the ACC is maximal when a low SLP is settled over the southern part of the Southern Ocean, particularly near 250-260^{o}E, and vice versa. As we saw before the region upstream of Drake Passage is important from the point of view of a balance between the wind stress and form stress in Drake Passage that impacts the variability of the meridional mass fluxes in the Pacific sector of the Southern Ocean. Therefore it is clear that a high atmospheric pressure settled over the upstream of Drake Passage region changes the above balance in Drake Passage, and together with the inverse barometer response to atmospheric pressure result in equatorward meridional flux anomaly in the Pacific sector of the Southern Ocean that, as was shown by Stepanov (2009 a,b), leads to conditions favourable to amplify warm ENSO. While a low pressure developed over this region "accelerates" the wind over the ACC leading to poleward meridional flux anomaly in the Pacific sector of the Southern Ocean resulting in the development of cold ENSO (Stepanov (2009 a,b)).

Figure 3 shows July-September (Fig. 3a-c) and August-October (Fig. 3d) mean ERAInterim SLP anomalies (from the 1989-2011 mean) that are typical before the maximum phase of the development of warm (Fig. 3a-b) and cold (Fig. 3c-d) ENSO events. Before warm ENSO reaches its maximum phase of development, over the region upstream/near of Drake Passage high atmospheric pressure is settled (Fig. 3a-b), while low SLP over this region is observed during the months preceding the maximum phase of the development of a cold ENSO (Fig. 3c-d). The lag between the changes of atmospheric conditions over the ACC and maximum phase of ENSO development (3-6 months) is in accordance with previous finding by Stepanov (2009a), e.g., the cold ENSO of 2007 has reached its maximum phase of the development about 1-2 months later than ones in 1997, 1998 and 2002 (Fig. 3a-c), therefore the negative SLP anomalies in the Southern Ocean near Antarctica have also been observed later (Fig. 3d). Similar distribution of SLP anomalies has also been observed 3-5 months before the development of maximal phase of the ENSO in 1992, 1994, 1995, 2000, 2002, 2004, 2006, 2007, 2008, 2009 and 2010. Thus we see that atmospheric pressure patterns near/upstream of Drake Passage region can be connected with ENSO events.

As was mentioned in Introduction SAM index and the variability of the oceanic mass in the Pacific sector of the Southern ocean are significantly negatively correlated with NINO4 index, however the correlation coefficient between SAM index and NINO4 index is low (~-0.2). Now when we realise that the atmospheric conditions over the region upstream of Drake Passage can be significant for ENSO development, we can choose some other index.

Near the western coast of South America at ~35°S there is a region of high atmospheric pressure (Fig. 2a) and an analysis of ERAInterim SLP shows that sometimes the area of high pressure penetrates to the south, in the region upstream of Drake Passage, between 260-290^{o}E. This path is in accordance with the preferred propagation away from the Southern Hemisphere subtropical jet waveguides indicated by Ambrizzi et al. (1995). Therefore the averaged sea level pressure anomaly along 280^{o}E between 35^{o}S (the point marked by black cross on Fig. 2c) and 45^{o}S, Δp, can be a good indicator for predicting such changes in atmospheric pressure field.

In introduction it was supposed that NINO4 describes a primary source of some factor forcing the maximal development of ENSO events, which is due to ocean impact (NINO4 is the region where changes of sea-surface temperature lead to total values around 27.5^{o}C, which is thought to be an important threshold in producing rainfall in the tropics during ENSO). Therefore model ocean characteristics obtained by Stepanov (2009a) have been compared with NINO4. However analysing SLP field, variability of which reflects joint effect of the interaction between the ocean and atmosphere, assumes using NINO index, incorporating similar impact. Therefore further we will compare new characteristics found with NINO3.4 index (SST averaged in area of 5^{o}-5^{o}S; 170-120^{o}W, www.cpc.ncep.noaa.gov/data/indices): it is the region that has large ENSO variability, and that is close to NINO4 region where changes in local sea-surface temperature are important for shifting the large region of rainfall typically located in the far western Pacific (though the comparison results are similar for NINO4 too).

Figure 4 shows normalized on their standard deviations anomalies monthly time series of NINO3.4 index (black dashed) and Δp (solid line) after applying 5 month running average procedure (this procedure minimizes intra-seasonal noise, e.g., see Trenberth, 1997, note that this smoothing leads to that time series of the SOI index correspond very well with changes in ocean temperatures across the tropical Pacific). The black solid line is after subtraction of the seasonal cycle and is shifted 4 months forward. One can see that there is correspondence between peaks and troughs of NINO-index with ones of Δp curve that have been observed 3-5 months before the maximum phase of the development of ENSO. The effect of atmospheric stochastic forcing, which always exists in the processes of the interaction between the atmosphere and the ocean, led to wider time lag (3-5 months) between atmospheric changes in the Southern Ocean and the maximum phase of the development of ENSO. The cases when NINO variability is in phase with/or slightly leads SLP ones are seen only in the middle of years (these events are not considered by the paper), while at the end/beginning of years (when the maximal developments of ENSO occur) SLP variability always leads NINO3.4 (exactly these cases are considered by the paper, i.e. we look at SLP change several months before maximal ENSO development).

The correlation coefficient between NINO3.4 index and Δp time series for 1989-2011 period is about 0.6 (Δp leads 4 months) and slightly varies for 1989-1999 (0.65) and 2000-2011 (~0.55) periods (tests to determine the significance of difference in correlations between two periods shows that this difference is not statistically significant). Later we will see that the EOF2 (Fig. 6b) captures a zonal dipole pattern near Drake Passage presented in Fig. 3, with PC2 that is generally bigger and maxima of PC2 are wider prior to the 2000s than after (the same is true for NINO4-index). Therefore the correlation coefficient between the two indices for the period prior to the 2000s can be slightly greater than one after 2000, but, as was mentioned above, the difference is not statistically significant.

Figure 5 shows 1989-1999 (a) and 2000-2008 (b) standard deviations of SLP from 10^{o}N to the Antarctic continent. One can see that atmospheric dynamics near Antarctica has not been substantially changed: only over the upstream of Drake Passage region a high variability of the SLP became more localized near Drake Passage, while in the tropical Pacific, the SLP variability decreased in the 2000s (Fig. 5c-d). Since the mid 1990s the SST became warmer, therefore if we exclude from consideration the effect of the tropical cyclones (they rarely form within 5° of the equator (Henderson-Sellers et al, 1998) and their impact is significant in the northwest Pacific Ocean basin only), it is reasonable to suppose that the variability of atmosphere in the tropics is decreased, which does not allow developing conventional ENSO (described by NINO3 index). Results presented on Fig. 5c-d confirm this conclusion: before 2000 the variability of the SLP over the tropical Pacific was higher than after: in the 2000s the atmospheric pressure patterns show weaker variability (~70% from 1989-2011 mean variability), while during the 1989-1999 period the area of higher atmospheric pressure variability (>100% of 1989-2011 mean one) occupied almost the whole tropical Pacific. However, the atmospheric variability in moderate and high latitudes of the southern hemisphere did not change noticeably (Fig. 5a-b), which suggests that the effect of processes near Antarctica still impact the tropical region of the Pacific Ocean with the same efficacy.

The interaction between the atmosphere and the ocean due to the existence of stochastic forcings (e.g., see Flügel et al. (2004), Eisenman et al. (2005)) limits the predictability of ENSO (especially “warm-pool El Niño”, e.g. see Horii et al. 2012). The stochastic variability can lead to some interannual changes in the tropics when weak tropical temperature anomalies can be superimposed leading to substantial changes in the atmospheric meridional circulation. An example is 2006 when a long warm period in the central tropics (during more than half of a year) provided discharged conditions of the recharge/discharge ENSO oscillator at the beginning of 2007 (Horii et al. (2012)).

This cooling in the tropics led to the intensification of the meridional atmospheric circulation cell and stronger wind over the ACC (the value of SAM index exceeded its standard deviation) when negative SLP anomaly developed over the Southern Ocean (Fig. 3d) that finally resulted in the development of the strong cold ENSO in 2007-2008. This ENSO had led to charged conditions of the recharge/discharge ENSO oscillator and, as a result, the atmospheric variability in the tropical Pacific has been increased after 2008. Figures 5 e-f show that 2000-2007 period had small SLP variability (Fig. 5e), but 2008-2011 SLP variability in the western tropical Pacific (Fig. 5f) is comparable with one before 2000 (Fig. 5c) that increases the impact of the tropical interactions on ENSO.

This variability is in agreement with NINO index variability. However, we should estimate the variability of the difference, e.g. between NINO3.4 and NINO4 indexes, rather than the change of absolute values themselves since the zonal gradient is significant for the intensity of Walker circulation, which can be characterized by SOI index. Analysis shows that really standard deviation of the difference between NINO3.4 and NINO4 for 1989-1999 period 2 times more than for 2000-2011. Besides, there is a significant correlation of the difference between NINO3.4 and NINO4 with SOI for 1989-1999 (-0.51), while the same correlation for 2000-2011 is about zero. Thus, the significant correlation before 2000 and zero ones after 2000 says that the contribution of atmospheric component of ENSO due to the variability of atmospheric forcing in the western equatorial Pacific reduced, and hence the variability over the Southern ocean recently can contribute more in the processes of ENSO developments than it was before the 2000s. It is worth noting also that the significant correlations between SOI and NINO3.4 (-0.84) and NINO4 (-0.79) for 2008-2011 period are higher than during 2000-2007 (-0.58 and -0.47, respectively for NINO3.4 and NINO4). The differences in correlations between two periods are statistically significant. The change of the above correlations is in agreement with results presented in Fig. 5 e-f. The above facts explain why the correlation between the SOI and NINO also remains statistically significant during warm periods. It is likely that during warm periods the atmospheric variability in the tropics will be decreased again after onsets of series of the “warm-pool El Niño” events.

3. The results of an EOF analysis of ERAInterim SLP field.

The EOF analysis of atmospheric pressure patterns in the SE Pacific revealed an additional mechanism explaining the change in ENSO characteristics in the 2000s. The first, second and fifth leading EOF modes of monthly SLP field over the region of the Southern Ocean in the area south of 31°S; 150-310°E are presented in Fig. 6a-c. The EOF1 pattern shown in Fig. 6a captures the almost zonal structure of the SLP over the ACC. This mode explains about of 44% of the total variability over the region for the period between 1989 and 2011. The EOF2 (Fig. 6b) that explains about 14% of the SLP variability captures a zonal dipole pattern near Drake Passage that is in accordance with Fig. 3. Finally, the EOF5 mode (Fig. 6c) explaining 5% of the SLP variability captures a meridional dipole pattern to the west of Drake Passage, which characterizes the variability of the strength of meridional shear of zonal wind.

The EOF3 (explains less than 10% of the total variability) is omitted from a consideration, since the EOF3 has a strong resemblance to the Pacific-South American pattern identified by Mo and Ghil (1987), with principal component PC3 slightly correlated with NINO index (the highest correlation (~0.3) corresponds to the case when NINO index leads PC3 by 3 months), and it is strongly associated with ENSO events (Sinclair et al. (1997); Carleton (2003)). The EOF4 (~7% of the total variability) is not considered here because of its some resemblance to the EOF2 (high/low pressure upstream and near of Drake Passage) and there is only a slight correlation between PC4 and NINO3.4 (~0.3) for 1989-2001 period with PC4 leading NINO3.4 at about 3-4 months (for 2002-2011 PC4 and NINO3.4 are not correlated at all, i.e. this mode cannot be a plausible reason for the change in ENSO characteristics in the 2000s).

The time series of the normalized principal components (PCs) of EOF1, EOF2 and EOF5 together with normalized NINO3.4 index are presented in Fig. 6d-f. A cross-correlation analysis between these PCs and NINO3.4 index at different leads and lags for 1989-2011 period gives a maximum correlations of 0.45, 0.55 and 0.38 with PCs leading NINO3.4 at 1, 4 and 8 months respectively for PC1, PC2 and PC5. However, we should note that correlations between PC1, PC2 and NINO3.4 for whole 1989-2011 period and for 2 subperiods (1989-2001 and 2002-2011 periods) are comparable (about 0.4 for PC1 and 0.5 for PC2), but the correlations between PC5 and NINO3.4 are different for these different periods. The 2002-2011 period is a major contributor to the value of correlation coefficient between PC5 and NINO3.4 for 1989-2011 period: 2002-2011 correlation is about 0.8, while for 1989-2001 PC5 and NINO3.4 are not correlated at all. As was mentioned earlier, the EOF5 characterizes the strength of meridional shear of zonal wind over the region under consideration, which defines the growth rate of the air jet instability over this region (see, e.g. Gill (1982), Paldor and Dvorkin (2006)). The high correlation between PC5 and NINO3.4 means that air jet instability over the region, leading to the formation of SLP patterns shown in Fig.3, became to be a significant contributor to the development of maximal phase of the ENSO after 2002 with lead time of about 8 months, i.e., this event is coincident with the time of ENSO onset, Larkin and Harrison (2005).

Of course, it does not mean that the after change of PC5 it is needed about 4 months to lead to the formation of SLP patterns shown in Fig.3. The PC5 variability shows only that 8 months before the development of maximal phase of the ENSO (i.e. in April, after boreal summer) there are atmospheric conditions over the south-east Pacific sector of the Southern ocean, which characterize higher meridional shear of zonal wind here. This variability is likely connected with global meridional atmospheric circulation change in this time. This higher meridional shear of zonal wind in April results in higher likelihood that the air jet instability will occur during Australian winter (July-September) when the maximal variability of atmospheric characteristics is observed.

Many authors accept to take into account EOF modes just up to the 4-th order and they assume that adding a few more does not modify the picture in any substantial way (e.g., see de Viron et al. (2013)), that choice is based on Monte Carlo tests done by Overland and Preisendorfer (1982), who showed that for their analysis only the first four PCs were significant. However, as follows from Overland and Preisendorfer (1982), the significance of EOF modes depends on both length of observation data set and the choice of a number of eigenvalue statistics, p. Therefore to check a significance of our 5-th EOF mode, Monte Carlo test has been done similar to Overland and Preisendorfer (1982). That is, it was verified if the eigenvalues of an EOF analysis of monthly SLP anomalies can be distinguished from those produced from spatially and temporally uncorrelated random process. A random number generator was used to produce uncorrelated gaussian variables of zero mean and unit variance and corresponding eigenvalues have been calculated (for computation of the covariance matrix the value of variance is irrelevant). The experiment has been repeated one hundred times. Let us denote by λ_j and δ_j^r eigenvalues computed from data sets corresponding to SLP field and r-th Monte Carlo experiment, respectively (where j ($j=1, \dots, p$) is j-th EOF mode). Then the rule N that was used by Overland and Preisendorfer (1982) to distinguish observed mode from those produced by random processes, is given by the following: terminate the sequence of the normalized eigenvalues T_j, which is:

$$T_j = \lambda_j \left(\sum_{j=1}^{p} \lambda_j\right)^{-1}, \; j=1, \dots, p, \qquad (1)$$

at the largest integer $j=m$ such that T_m exceeds U_m^{95}, where U_m^{95} is normalized eigenvalue calculated for random processes so that for fixed j we have the following order: $U_j^1 \leq U_j^2 \leq \dots \leq U_j^{100}$, where

$$U_j^r = \delta_j \left(\sum_{j=1}^{p} \delta_j^r\right)^{-1}, \; j=1, \dots, p, \quad r=1, \dots, 100. \qquad (2)$$

Table 1 lists the normalized eigenvalues, T_j, and the ratio, T_j/U_j^{95}, which determines the application of rule N, for two choices of value of p. Both choices of p are sensible. The choice of p=22 corresponds to the case when the first 22 EOF's modes explain about of 98% of the total SLP variability over the region for the period between 1989 and 2011. While the choice of p=45 is based on sampling "stochastic" eigenvalues with maximal values: each from the first 45 EOF's modes explains approximately the same value of the total stochastic variability (cumulatively they explain only about of 20% of the total stochastic variability). Perhaps, the second choice is more adequate. Note here that Overland and Preisendorfer (1982) have used higher values for p: 56 and 74. Thus, the first five EOF's appear to contain meteorological information distinguished from noise, based upon rule N, and the use of this mode in our analysis is justified.

The EOF analysis agrees with the previous cross-correlation analysis. So, PC1 is highly correlated with SAM index (with coefficient about -0.9) since EOF1 and SAM index describe the weakness and strength of wind over the ACC respectively. The EOF2 is in a good agreement with SLP anomaly pattern near Drake Passage presented in Fig. 3. Both Δp and PC2 are significantly correlated with NINO3.4 (with the coefficient of ~0.6 and 0.5 respectively) with lead time of about 4 months.

4. Discussion and conclusions

It is a generally accepted opinion that ENSO events are caused by the interaction processes between the ocean and atmosphere in the tropics (excluding the recent paper by Terray (2011) who pointed out the linkage between mid-latitude Southern Hemisphere climate and ENSO). It is well known that the onset of ENSO events depends on the type of wind anomalies that are established in the western equatorial part of the Pacific Ocean in the previous spring and summer. However, it was shown by Lengaigne et al. (2004), these wind anomalies can trigger ENSO only under particular favourable oceanic conditions. It was demonstrated by Eisenman et al. (2005) that the wind anomalies considered in the tropics are a combination of joint effects of stochastic atmospheric forcing and large-scale dynamics depending on the ENSO processes rather than being completely external to the development of the ENSO events. Recently, Horii et al. (2012) have demonstrated that because of some decadal changes in the variability of warm water volume of the equatorial Pacific and wind variability in the western equatorial Pacific the robust predictability of these two predictors for ENSO has changed in the 2000s: the lead time of two to three seasons observed before 2000 has almost vanished and in the 2000s the variability of the warm water volume of the equatorial Pacific and wind variability in the western equatorial Pacific occur almost in phase with ENSO development. This suggests that other factors can impact the ENSO onsets.

This paper has considered a hypothesis based on the numerical results by Stepanov (2009 a,b) that the atmospheric variability over the ACC can strongly influence amplifying ENSO events. This hypothesis allows us to explain the breakdown in the 2000s of ENSO predictors proposed by McPhaden (2003) through analysis of SLP fields. It was shown that the maximum phase of the development of most ENSO events was associated with a change of the atmospheric conditions upstream of Drake Passage in July-October when the variability of the atmosphere over the Southern Ocean is especially strong. This variability, together with the effect of the bottom topography, leads to the changes of the balance between the wind stress and form stress in Drake Passage that, together with the inverse barometer response to atmospheric pressure, result in the appearance of anomalies in the fields of the pressure and density in the Southern Ocean. By means of the wave mechanism described by Ivchenko et al. (2004, 2006) and Blaker et al (2006), these anomalies can be transported to the low latitudes of the Pacific ocean, where they interact with the stratification via Kelvin wave propagation and can cause variations in the inclination of the thermocline in the tropical Pacific, which, in turn, can amplify ENSO event (Stepanov (2009 a,b)). In the 2000s, due to warmer SST, more homogeneous dynamical conditions in the tropics developed (Fig. 5d), hence the subsequent interaction between the atmosphere and ocean in the tropics after the beginning of ENSO in the central equatorial Pacific is suppressed and a strong ENSO cannot be developed in the eastern side of the tropical Pacific. As a result, frequent occurrences of the “warm-pool El Niño”, which is characterized by SST anomalies centered in the central equatorial Pacific, are observed (Horii et al. (2012)). The high correlation between PC5 and NINO after 2002, EOF5 of which characterizes the strength of the meridional shear of zonal wind over the region under consideration, demonstrates that during warm periods the air jet instability over the region significantly impact ENSO. Due to this instability in the region to the west of Drake Passage, anticyclonic/cyclonic atmospheric circulation patterns can arise. It is likely that due to air jet instability during cold periods (when the meridional shear of zonal wind is stronger) the area with high atmospheric pressure can be developed over the region upstream of Drake Passage more frequently, therefore generally more warm ENSO events than cold ones are observed. For example, the Oceanic Niño Index from http://www.cpc.ncep.noaa.gov/products/analysis_monitoring/ensostuff/ensoyears.shtml. This shows that for 1950-2002 period 15 warm and 11 cold ENSO events have been observed respectively, while after 2002 the numbers of warm and cold ENSO were the same. It is in agreement with the analysis of PC2 and PC5 timeseries. Both timeseries are not symmetric with respect to the zero value. The skewness coefficients for the unsmoothed PC2 and PC5 timeseries for the period of 1989-2011 are about 0.2, and about 2 times greater for the period before 2000. The positive value of the skewness indicates that more often SLP anomalies, having constituents similar to EOF2 and EOF5 patterns presented in Fig. 6 b,c, can be developed in the region under consideration.

The EOF analysis has revealed the best possible ENSO predictor for warm periods: it is PC5 that is highly correlated with NINO3.4 (~0.8) with lead time of 8 months. It means that processes in the Southern Ocean due to air jet instability over the ACC during warm periods significantly contribute to development of maximal phase of ENSO. One might argue that the conclusion stands on the principle component PC5 which has only 5% of total variance, and even if the PC5 correlates well with ENSO with a 8-month lead, we cannot suggest that the SLP anomalies over the Southern Ocean could have very significant effect on ENSO. However, it is well known that extreme events are described by “probability distribution tail” that describes even less than 5% of all possible outcomes (and ENSO can be considered such an event, since no regularity for ENSO events is observed because the wind anomalies considered in the tropics are a combination of joint effects of stochastic atmospheric forcing and large-scale dynamics (Eisenman et al. (2005)). It is worth noting that the pressure difference between centres of regions with high and low pressure of EOF5 mode (Fig. 6c) is more than 50% of a similar difference of EOF1 mode (Fig.6a). Thus PC5 describing only 5% of total variance of SLP field can be significant for ENSO forecast since it describes an appearance of plausible favourable conditions resulting in air jet instability over the ACC that leads to different July-September SLP patterns in the Southern Ocean (characterized by EOF2, explaining 14% of total variance).

As was noted in the Introduction ENSO events could be considered as a consequence of changes in the global meridional atmospheric circulation when the tropics and high latitudes interact with each other rather than a local phenomenon. Since the interaction between the tropics and high latitudes depends on the stochastic processes, which always occur during the interaction between the atmosphere and the ocean, time lag between atmospheric changes in the Southern Ocean and the maximum phase of the development of ENSO is in a wide range of 3-5 months. Note here that the primary component of stochastic forcing can be tropical intraseasonal variation, such as the Madden–Julian Oscillation (MJO), Madden and Julian (1972), since MJO can impact the development ENSO from the surface; it is likely that local atmospheric forcing is important to this type of ENSO, such as those associated with the MJO. However, it is worth noting that Stepanov and Hughes (2006) have shown that large-scale mass exchange exists not only between the Southern Ocean and Pacific. There are also the Atlantic-Pacific and slightly weaker Indian-Pacific exchanges at shorter timescales (periods from few days to 3 months). Therefore it is likely that this exchange can lead to the appearance of some signals in the tropics and mid-latitudes of the Indian and Atlantic oceans too. Hints of this can be seen in Fig. 7 presented by Stepanov (2009a) showing the model temperature anomaly on the zonal section along the equator for the Indian Ocean too, which are due to the variability of wind forcing over the ACC, together with the effect of bottom topography, though in this experiment the forcing was defined as velocity disturbance for the meridional component of the velocity only in the Pacific sector of the Southern ocean. It is likely that MJO and, e.g., subtropical dipole variability in both the Southern Indian and Atlantic Oceans triggered by Southern Hemisphere mid-latitude variability influencing ENSO found by Terray (2011), are the results of such global inter-basin mass exchange. Further studies are needed to explore this hypothesis.

During warmer periods, meridional gradients of the atmospheric dynamic characteristics that describe inter-latitudinal exchange, are weaker, therefore the SLP variability in the tropics becomes weaker leading to the development of frequent but weak ENSO events (with SST anomalies centered in the central equatorial Pacific). Interestingly, the observed result of frequent occurrence of the "warm-pool El Niño" in the 2000s is consistent with coupled model simulations under global warming by Yeh et al. (2009).

In conclusion, it is worth noting that the results of the paper are in good agreement with Byshev et al., (2012). They showed that the warm ENSO events are accompanied by the global atmospheric oscillation when high atmospheric pressure is generated in the equatorial-tropical latitude band (~45^0N - 45^0S; 60^0W-180^0), and a low atmospheric pressure develops over 2-3×10^3 km zone along the outer boundaries of that structure. Thus, the magnitude of the meridional gradient of the zonal wind speeds over the Southern Ocean is increasing, and favourable conditions for the onset of instability of the air jet over the ACC are created leading to the appearance of blocking anticyclone over the south-eastern part of the Pacific sector of the Southern Ocean. In the northern hemisphere, the changes in the atmosphere, described by Byshev et al., (2012), may also lead to the appearance of SST anomalies in the western North Pacific, which, according to Wang et al. (2012), can trigger oceanic Kelvin waves, which propagate eastward and initiate the developments of ENSO.

Acknowledgements. The author would like to thank Keith Haines for his support in doing the work. Thanks to Dr. N.Howe who carefully read the draft of the paper and provided helpful comments. Comments from two anonymous reviewers helped to significantly improve the manuscript. This work was supported by the NCEO and the RAPID -Watch Valor projects.

References

1. Alexander, M. A., L. Matrosova, C. Penland, J. D. Scott, and P. Chang (2008), Forecasting Pacific SSTs: Linear inverse model predictions of the PDO, J. Clim., 21, 385–402, doi:10.1175/2007JCLI1849.1.
2. Ambrizzi T., B.J. Hoskins and H.-H. Hsu (1995), Rossby wave propagation and teleconnection patterns in austral winter, J. Atmos. Sci. 52(21), DOI: 10.1175/1520-0469(1995) 052<3661:RWPATP>2.0.CO;2
3. Ashok, K., S. K. Behera, S. A. Rao, H. Weng, and T. Yamagata (2007), El Niño Modoki and its possible teleconnection, J. Geophys. Res., 112, C11007, doi:10.1029/2006JC003798.
4. Blaker, A.T., B. Sinha, V.O. Ivchenko, N.C. Wells, and V.B. Zalesny (2006) Identifying the roles of the ocean and atmosphere in creating a rapid equatorial response to a Southern Ocean anomaly, Geophysical Research Letters, v.33, L06720, doi:10.1029/2005GL025474.
5. Bretherton, C. S., M. Widmann, V.P. Dymnikov, J. M. Wallace, and I. Bladė (1999) The effective number of spatial degrees of freedom of a time-varying field, J. Climate, 12(7), 1990-2009.
6. V.I.Byshev, V.G.Neyman, Yu.A.Romanov and I.V.Serykh, El Niño as a consequence of the Global Oscillation in the dynamics of the Earth’s climate system// Doklady Earth Sciences, 2012, vol. 446, Part 1, pp. 1089-1094.
7. Carleton A.M (2003), Atmospheric teleconnections involving the Southern Ocean, J. of Geophysical Research, 108(C4), DOI: 10.1029/2000JC000379.
8. Chang, P., L. Zhang, R. Saravanan, D. J. Vimont, J. C. H. Chiang, L. Ji, H. Seidel, and M. K. Tippett (2007), Pacific meridional mode and El Niño–Southern Oscillation, Geophys. Res. Lett., 34, L16608, doi:10.1029/2007GL030302.
9. Clarke, A. J., and S. Van Gorder (2003) Improving El Niño prediction using a space-time integration of Indo-Pacific winds and equatorial Pacific upper ocean heat content, Geophys. Res. Lett., 30(7), 1399, doi:10.1029/2002GL016673.

10. de Viron O., J. O. Dickey, and M. Ghil (2013), Global modes of climate variability, Geophys. Res. Lett., 40, 1832–1837, doi:10.1002/grl.50386.

11. Dong, B., R.T. Sutton, and A.A. Scaife (2006) Multidecadal modulation of El Niño-Southern Oscillation (ENSO) variance by Atlantic Ocean sea surface temperatures, Geophysical Research Letters, v.33, L08705, doi:10.1029/2006GL025766.

12. Eisenman I., L. Yu, E. Tziperman (2005) Westerly Wind Bursts: ENSO's tail rather than the dog?, J. Climate, 18, 5224-5238.

13. Flügel M., P. Chang, C. Penland (2004) The role of stochastic forcing in modulating ENSO predictability, J. Climate, 17, 3125-3140.

14. Gill, A. E., 1982: Atmosphere–Ocean Dynamics. Academic Press, 662 pp.

15. Henderson-Sellers A., H. Zhang, G. Berz, K. Emanuel, W. Gray, C. Landsea, G. Holland, J. Lighthill, S-L. Shieh, P. Webster, and K. McGuffie (1998) Tropical cyclones and global climate change: A post-IPCC assessment, Bulletin of the American Meteorological Society 79(1), p.19-38. doi: http://dx.doi.org/10.1175/1520-0477(1998)079<0019:TCAGCC>2.0.CO;2.

16. Horii T., I. Ueki, and K. Hanawa (2012) Breakdown of ENSO predictors in the 2000s: Decadal changes of recharge/discharge-SST phase relation and atmospheric intraseasonal forcing, Geophys. Res. Lett., 39, L10707, doi:10.1029/2012GL051740.

17. Ivchenko V.O., V. B. Zalesny, and M.R. Drinkwater (2004) Can the equatorial ocean quickly respond to Antarctica sea ice/salinity anomalies?, Geophysical Research Letters, v.31, L15310, doi:10.1029/2004GL020472.

18. Ivchenko V.O., V. B. Zalesny, and M.R. Drinkwater and J. Schröter (2006) A quick response of the equatorial ocean to Antarctic sea ice/salinity anomalies, J. of Geophysical Research, vol. 111, C10018, doi:10.1029/2005JC003061.

19. Jin, F.-F. (1997) An equatorial recharge paradigm for ENSO. Part I: Conceptual model. J. Atmos. Sci., 1997, V.54, p. 811–829.

20. Kao, H.-Y., and J.-Y. Yu, 2009: Contrasting eastern-Pacific and central-Pacific types of ENSO. J. Climate, 22, 615–632.

21. Kug, J.-S., F.-F. Jin, and S.-I. An (2009), Two types of El Niño events: Cold Tongue El Niño and Warm Pool El Niño, J. Clim., 22, 1499–1515, doi:10.1175/2008JCLI2624.1.

22. Larkin, N. K., and D. E. Harrison (2005), Global seasonal temperature and precipitation anomalies during El Niño autumn and winter, Geophys. Res. Lett., 32, L16705, doi:10.1029/2005GL022860.

23. Lau N.-C., A. Leetmaa, M.J. Nath, H.-L. Wang (2005) Influence of ENSO-induced Indo-Western Pacific SST anomalies on extratropical atmospheric variability during the boreal summer, Climate, 18, 2922-2942.

24. Lee, T., and M. J. McPhaden (2010), Increasing intensity of El Niño in the central-equatorial Pacific, Geophys. Res. Lett., 37, L14603, doi:10.1029/2010GL044007.

25. Lengaigne M., E. Guilyardi, J.-P. Boulanger, C. Menkes, P. Delecluse, P. Inness, J.Cole, J. Slingo (2004) Triggering of El Niño by westerly wind events in a coupled general circulation model, Climate Dynamics, 23, 601-620, doi:10.1007/s00382-004-0457-2.

26. Madden, R. A., and P. R. Julian (1972), Description of global scale circulation cells in the tropics with a 40–50-day period, J. Atmos. Sci., 29, 1109–1123, doi:10.1175/1520-0469(1972)029<1109:DOGSCC>2.0.CO;2.

27. McPhaden, M. J. (2003) Tropical Pacific Ocean heat content variations and ENSO persistence barriers, Geophys. Res. Lett., 30(9), 1480, doi:10.1029/2003GL016872.

28. McPhaden, M. J., X. Zhang, H. H. Hendon, and M. C. Wheeler (2006) Large-scale dynamics and MJO forcing of ENSO variability, Geophys. Res. Lett., 33, L16702, doi:10.1029/2006GL026786.

29. Mo K.C. and M. Ghil (1987), Statistics and dynamics of persistent anomalies, J. Atmos. Sci., 44(5), DOI:10.1175/1520-0469(1987)044<0877:SADOPA>2.0.CO;2

30. Mokhov I.I., and D.A. Smirnov (2006) El Niño-Southern Oscillation drives North Atlantic Oscillation as revealed with nonlinear techniques from climatic indices, Geophysical Research Letters, v.33, L03708, doi:10.1029/2005GL024557.

31. Müller W.A., and E. Roecker (2006) ENSO impact on midlatitude circulation patterns in future climate change projections, Geophysical Research Letters, v.33, L05711, doi:10.1029/2005GL025032.

32. Nicholls N., H.-J. Baek, A. Gosai, L.E. Chambers, Y. Choi, D. Collins, P.M. Della-Marta, G.M. Griffiths, M.R. Haylock, N. Iga, R. Lata, L. Maitrepierre, M.J. Manton, H. Nakamigawa, N. Ouprasitwong, D. Solofa, L. Tahani, D.T. Thuy, L. Tibig, B.Trewin, K. Vediapan, and P. Zhai (2005) The El Niño-Southern Oscillation and daily temperature extremes in east Asia and the west Pacific, Geophysical Research Letters, v.32, L16714, doi:10.1029/2005GL022621.

33. Overland, J. E., and R.W. Preisendorfer (1982), A significance test for principal components applied to cyclone climatology, Mon. Wea. Rev., 110, 1–4.

34. Paldor N., and Y. Dvorkin (2006) Barotropic Instability of a Zonal Jet: From Nondivergent Perturbations on the β-Plane to Divergent Perturbations on a Sphere, J. Phys. Oceanogr., 36, 2271-2282.

35. Pierce, D. W., T. P. Barnett, and M. Latif (2000), Connections between the Pacific Ocean tropics and midlatitudes on decadal timescales, J. Clim., 13, 1173–1194, doi:10.1175/1520-0442(2000)013<1173:CBTPOT>2.0.CO2.

36. Sinclair M.R, J.A. Renwick and J.W. Kidson (1997), Low-Frequency Variability of Southern Hemisphere Sea Level Pressure and Weather System Activity, Mon Wea Rev, 125(10), DOI: 10.1175/1520-0493(1997)125<2531:LFVOSH>2.0.CO;2.

37. Stepanov V.N. and C.W. Hughes (2006) Propagation of signals in basin-scale bottom pressure from a barotropic model, J. Geophys. Res., 111, C12002, doi:10.1029/2005JC003450.

38. Stepanov V.N. (2009a) The meridional transport fluctuations in the Southern Ocean and its link with the ENSO events. Oceanology, Vol. 49, No. 1, pp. 5–19

39. Stepanov V.N. (2009b) The modelling of the ENSO events using a simple model. Oceanology, Vol. 49, No. 3, pp. 310–319.

40. Stepanov V.N., H. Zuo, K. Haines (2012) The link between the Barents Sea and ENSO events simulated by NEMO model. Ocean Sciences, 8, 971–982, doi:10.5194/os-8-971-2012.

41. Terray P. (2011) Southern Hemisphere extra-tropical forcing: a new paradigm for El Niño - Southern Oscillation, Clim Dyn (2011) 36:2171–2199, DOI 10.1007/s00382-010-0825-z.

42. Trenberth K.E. 1997. The definition of El Niño. Bulletin of the American Meteorological Society 78(12): 2771–2777.

43. Vimont, D. J., J. M. Wallace, and D. S. Battisti (2003a), The seasonal footprinting mechanism in the Pacific: Implications for ENSO, J. Clim., 16, 2668–2675, doi:10.1175/1520-0442(2003)016<2668:TSFMIT>2.0.CO2.

44. Vimont, D. J., D. S. Battisti, and A. C. Hirst (2003b), The seasonal footprinting mechanism in the CSIRO general circulation models, J. Clim., 16, 2653–2667, doi:10.1175/1520-0442(2003)016<2653:TSFMIT>2.0.CO2.

45. Wang S.-Yu, M. L'Heureux, and H.-H. Chia (2012) ENSO prediction one year in advance using western North Pacific sea surface temperatures, Geophys. Res. Lett., 39, L05702, doi:10.1029/2012GL050909.

46. Yeh, S.-W., J.-S. Kug, B. Dewitte, M.-H. Kwon, B. Kirtman, and F.-F. Jin (2009), El Niño in a changing climate, Nature, 461, 511–514, doi:10.1038/nature08316.

List of Figure Captions

Fig. 1. 1989-2009 correlations of zonally averaged sea level pressure with SOI-index with negative signs (a), and (b) with the zonally averaged sea level pressure difference between 17^{o} and 12^{o}S. Positive lags means that the zonally averaged sea level pressure lags from corresponding time series. (c) – time series of SOI-index with negative signs (red), zonally averaged sea level pressure difference between 17^{o} and 12^{o}S (blue), and zonally averaged sea level pressure difference between 17^{o} and the equator (green); d) – the same as c) but the seasonal cycle was removed and low-pass filtering with periods longer than 18 months was applied.

Fig. 2. 1989-2011 mean (a) and standard deviation (b) of sea level pressure, and correlations (c) between SAM index and sea level pressure for the same period. The dashed black line on Fig. 2c shows a zone of divergence (convergence) of the meridional mass fluxes according to Stepanov (2009a). The black cross denotes the position (280^{o}E and 35^{o}S) chosen to monitor the sea level pressure variability.

Fig. 3. Sea level pressure anomaly (in HPa) for July-September mean of 1997 (a), 2002 (b), 1998 (c) and for August-October mean of 2007 (d) before the maximum phase of the development of warm (a, b) and cold (c, d) ENSO.

Fig. 4. Normalized on their standard deviations anomalies monthly time series of NINO3.4 index (black dashed) and the averaged sea level pressure along 280^{o}E between 35^{o}S (the point marked by black cross on Fig. 4c) and 45^{o}S, Δp, (solid). The black solid line is after applying 5 month running average procedure and it is shifted 4 months forward; the seasonal cycle was subtracted.

Fig. 5. 1989-1999 (a) and 2000-2008 (b) standard deviations of sea level pressure (in Hpa); c-d – the same as a-b, but normalized on 1989-2011 mean standard deviations, and shown in enlarged scale for the tropics; e-f the same as c-d but for 2000-2007 and 2008-2011 periods respectively.

Fig. 6. EOF1 (a), EOF2 (b) and EOF5 (c) modes of the Southern ocean region SLP (1989-2011) multiplied by respective standard deviations of the principal components (units in Hpa). Normalized time series (solid line) of PC1 (d), PC2 (e) and PC5 (f) together with the time series of the NINO3.4 index (dashed line, after applying 5 month running average procedure) are also shown. PC1, PC2 and PC5 are after applying 5 month running average procedure and they are shifted forwards by 1, 4 and 8 months respectively.

Table 1. Summary of normalized eigenvalues. Rule N for selection of geophysical eigenvalues is satisfied for values of $T_j/U_j^{95} > 1$ (T_j satisfied rule N are presented by bold font)

	j					
	1	2	3	4	5	6
$T_j \times 100, p=22$	**45.5**	**14.3**	**10.1**	**7.5**	**5.2**	3.7
$T_j/U_j^{95}, p=22$	9.57	3.05	2.16	1.61	1.11	0.80
$T_j \times 100, p=45$	**44.8**	**14.1**	**10.0**	**7.4**	**5.1**	**3.7**
$T_j/U_j^{95}, p=45$	18.66	5.96	4.22	3.13	2.17	1.56

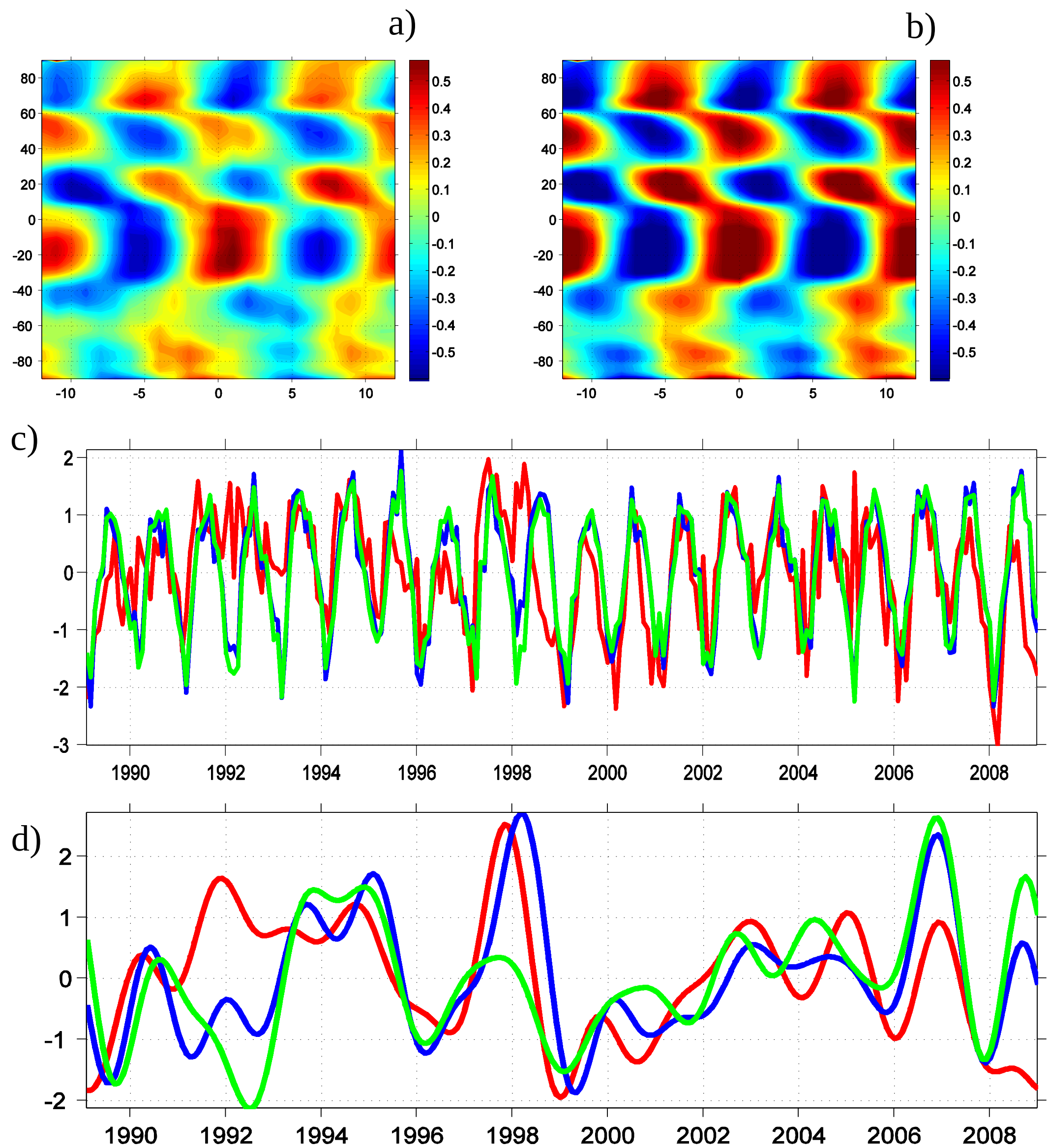

Fig. 1. 1989-2008 correlations of zonally averaged sea level pressure with SOI-index with negative signs (a), and (b) with the zonally averaged sea level pressure difference between 17^{o} and 12^{o}S. Positive lags means that the zonally averaged sea level pressure lags from corresponding time series. (c) – time series of SOI-index with negative signs (red), zonally averaged sea level pressure difference between 17^{o} and 12^{o}S (blue), and zonally averaged sea level pressure difference between 17^{o} and the equator (green); d) – the same as c) but the seasonal cycle was removed and low-pass filtering with periods longer than 18 months was applied.

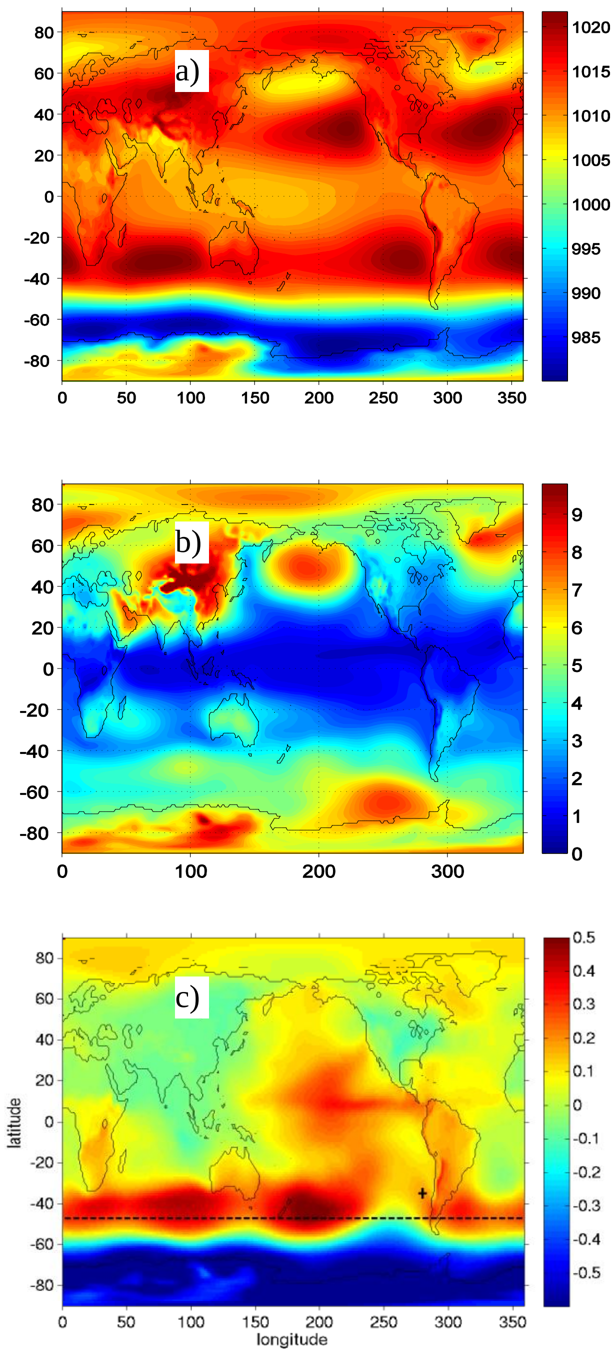

Fig. 2. 1989-2011 mean (a) and standard deviation (b) of sea level pressure and correlations (c) between SAM index and sea level pressure for the same period. The dashed black line on Fig. 2c shows a zone of divergence (convergence) of the meridional mass fluxes according to Stepanov (2009a). The black cross denotes the position (280^{o}E and 35^{o}S) chosen to monitor the sea level pressure variability.

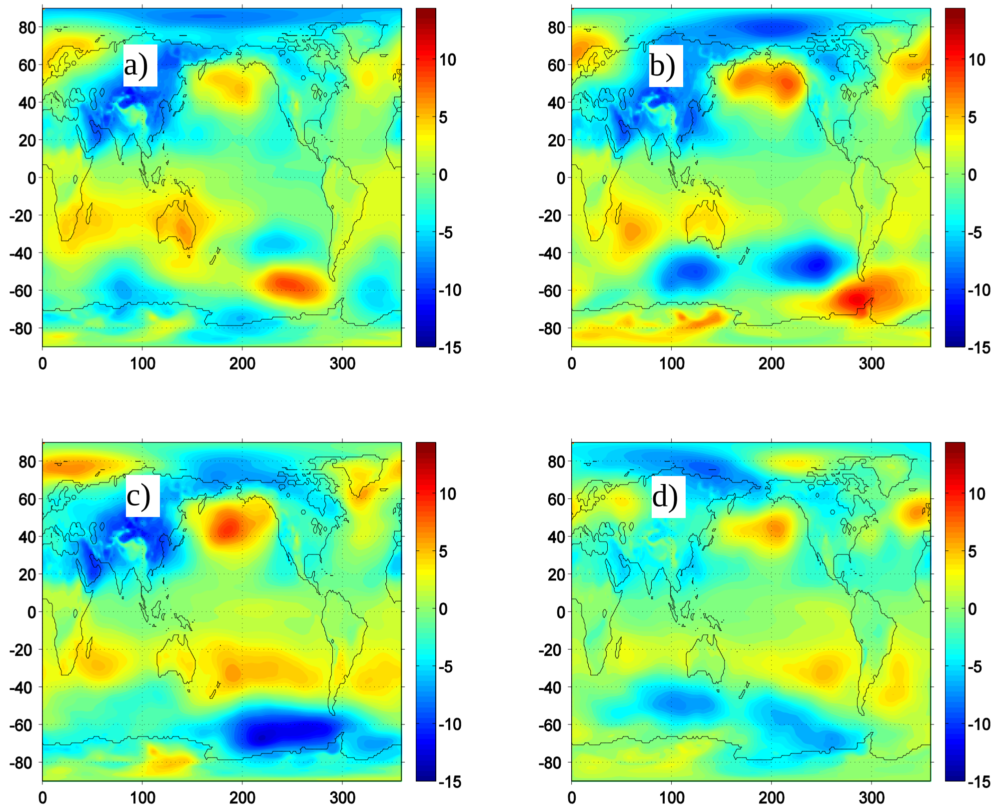

Fig. 3. Sea level pressure anomaly (in HPa) for July-September mean of 1997 (a), 2002 (b), 1998 (c) and for August-October mean of 2007 (d) before the maximum phase of the development of warm (a, b) and cold (c, d) ENSO.

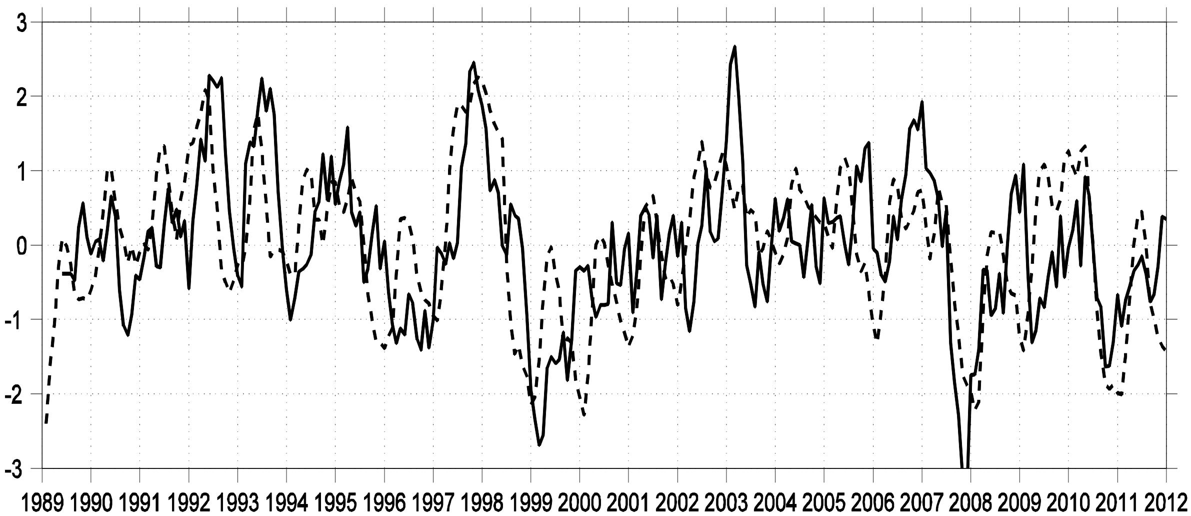

Figure 4. Normalized on their standard deviations anomalies monthly time series of NINO3.4 index (black dashed) and the averaged sea level pressure along 280^oE between 35^oS (the point marked by black cross on Fig. 5c) and 45^oS, Δp, (solid). The black solid line is after applying 5 month running average procedure and it is shifted 4 months forward; the seasonal cycle was subtracted.

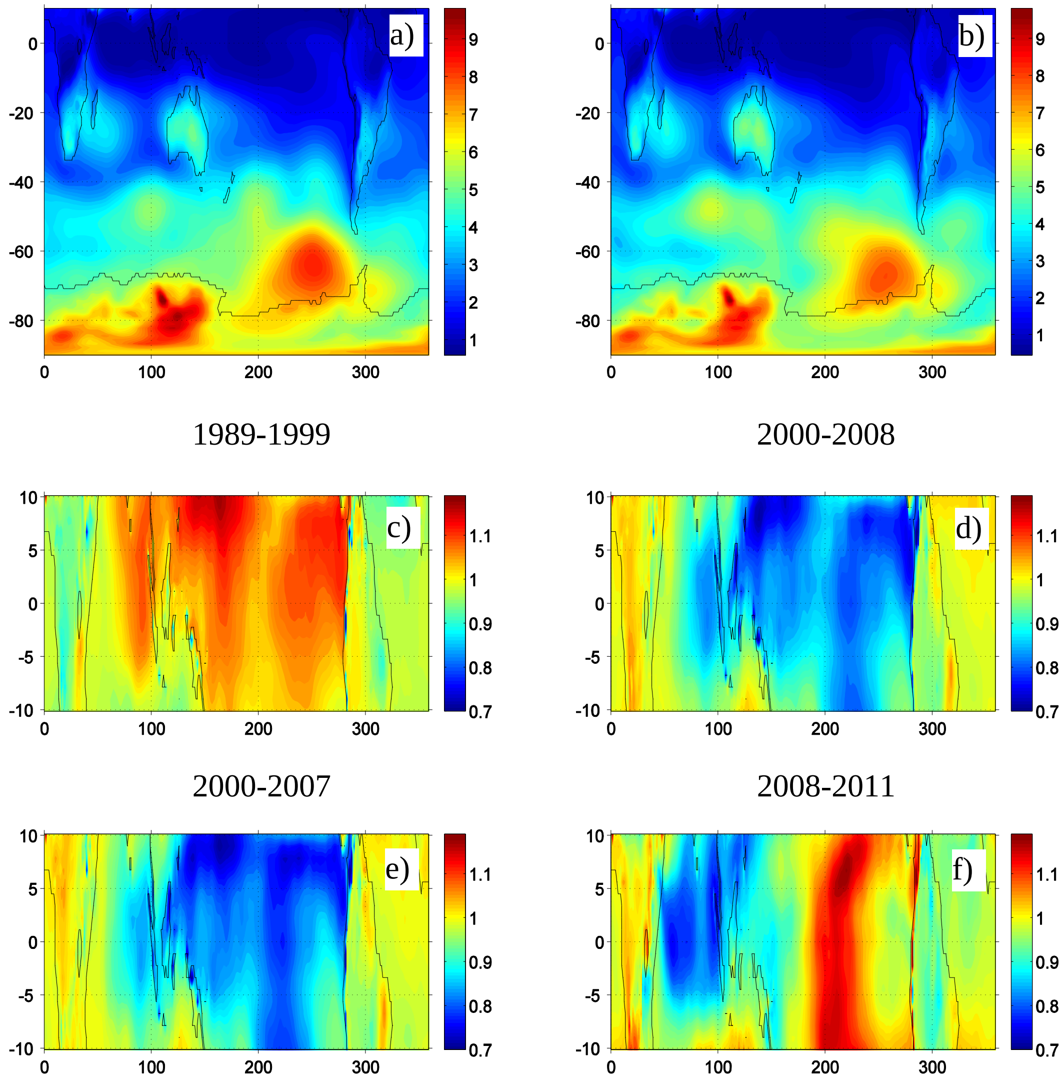

Fig. 5. 1989-1999 (a) and 2000-2008 (b) standard deviations of sea level pressure (in Hpa); c-d – the same as a-b, but normalized on 1989-2011 mean standard deviations, and shown in enlarged scale for the tropics; e-f the same as c-d but for 2000-2007 and 2008-2011 periods respectively.

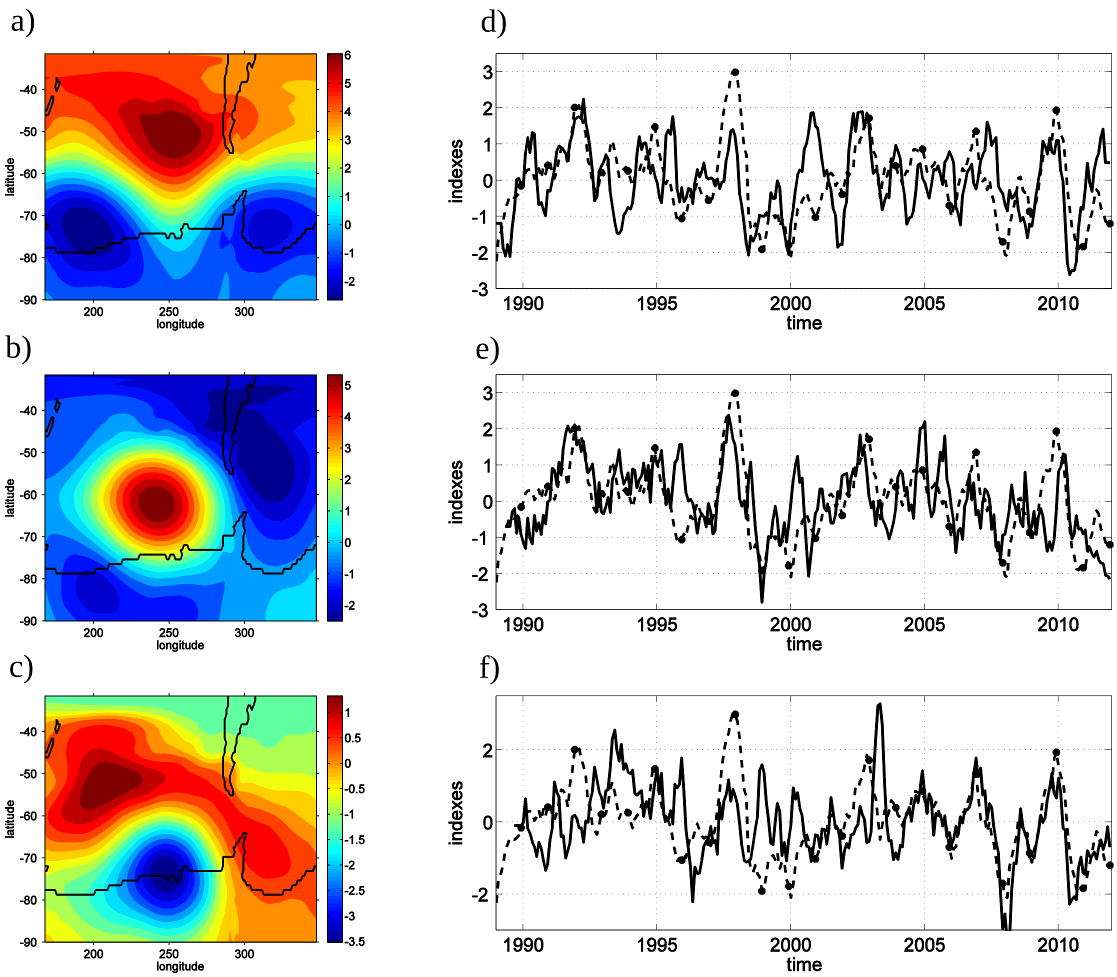

Fig. 6. EOF1 (a), EOF2 (b) and EOF5 (c) modes of the Southern ocean region SLP (1989-2011) multiplied by respective standard deviations of the principal components (units in Hpa). Normalized time series (solid line) of PC1 (d), PC2 (e) and PC5 (f). Also shown is the time series of the NINO3.4 index (dashed line). PC1, PC2 and PC5 are after applying 5 month running average procedure and they are shifted forwards by 1, 4 and 8 months respectively.